THE JOURNAL OF PHYSICAL CHEMISTRY Letters

Letter

pubs.acs.org/JPCL

Bright Photon Upconversion on Composite Organic Lanthanide Molecules through Localized Thermal Radiation

Huanqing Ye,[#] Viktor Bogdanov,[#,⊥] Sheng Liu,[#] Saumitra Vajandar,[†] Thomas Osipowicz,[†] Ignacio Hernández,[‡,⊗] and Qihua Xiong*[,#,∥,§]

[#]Division of Physics and Applied Physics, School of Physical and Mathematical Sciences, Nanyang Technological University, 21 Nanyang Link, 637371 Singapore

[⊥]Chemistry Department, M. V. Lomonosov Moscow State University, Leninskie Gory, 1-3, 119991, Moscow, Russia

[†]Centre for Ion Beam Applications, Department of Physics, Faculty of Science, National University of Singapore, 2 Science Drive 3, 117542 Singapore

[‡]Dpto. CITIMAC, Facultad de Ciencias, Universidad de Cantabria, Avda. Los Castros, s/n 39005 Santander, Spain

[⊗]Materials Research Institute and School of Physics and Astronomy, Queen Mary University of London, Mile End Road, London E1 4NS, United Kingdom

[∥]NOVITAS, Nanoelectronics Center of Excellence, School of Electrical and Electronic Engineering, Nanyang Technological University, 639798 Singapore

[§]MajuLab, CNRS-UNS-NUS-NTU International Joint Research Unit, UMI 3654, Singapore

Supporting Information

ABSTRACT: Converting low-energy photons via thermal radiation can be a potential approach for utilizing infrared (IR) photons to improve photovoltaic efficiency. Lanthanide-containing materials have achieved great progress in IR-to-visible photon upconversion (UC). Herein, we first report bright photon, tunable wavelength UC through localized thermal radiation at the molecular scale with low excitation power density (<10 W/cm^2) realized on lanthanide complexes of perfluorinated organic ligands. This is enabled by engineering the pathways of nonradiative de-excitation and energy transfer in a composite of ytterbium and terbium perfluoroimidodiphosphinates. The IR-excited thermal UC and wavelength control is realized through the terbium activators sensitized by the ytterbium sensitizers having high luminescence efficiency. The metallic molecular composite thus can be a potential energy material in the use of the IR solar spectrum for thermal photovoltaic applications.

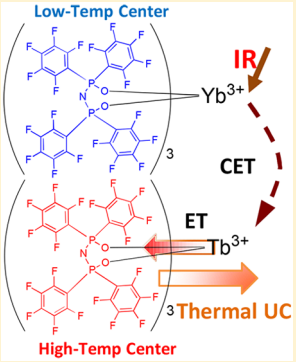

The solar spectrum contains a large portion of infrared (IR) photons that are below the band gap of most photovoltaic (PV) semiconductor materials. Thus, they cannot be absorbed by a single-junction PV device. Converting IR photons to visible photons the energies of which are above the PV material band gap would be a solution.[1,2] Lanthanide-based materials are mostly used for photon UC through excited-state absorption (ESA) or energy transfer upconversion (ETU).[3,4] ETU is termed as cooperative energy transfer (CET) if simultaneous sensitization is achieved in one activator from two sensitizers.[5−7] However, the problems of weak lanthanide absorption and weakly doped concentration give only weak UC brightness. Thermal radiation-induced photon UC has been recently demonstrated in weakly lanthanide-doped inorganic oxides as a bright alternative.[8,9] This mechanism occurs as a consequence of the IR absorption heating the materials through nonradiative multiphonon relaxation results in substantial thermal (blackbody type) radiation. Then, the extracted high-energy photons are emitted in a range that can be absorbed by commercial PV devices, potentially delivering cost-effective thermal PV devices to exceed the efficiency limit.[10,11] However, nonradiative processes with the potential to heat materials are reduced in lanthanide-based inorganics with long lanthanide emission lifetimes of a few milliseconds. Hence, thermal radiation-induced UC requires high excitation power density over 200 W/cm^2.[8] Moreover, for eliminating thermal loss, low thermal conductivity of the inorganics must be used, but the material choices are quite limited and the bulk inorganic crystals have to be cracked,[8,9,12] implying difficulty in developing them into realistic thermal PV devices.

Organic lanthanide materials would have important advantages: Organic lanthanide molecules reduce the ion trapping centers, thus increasing the lanthaide doping concentration. Intense organic ligand vibrations, which in fact prevent typically any use in UC-related applications, provide diverse nonradiative relaxation channels to deexcite the lanthanide excitations.[13,14]

Received: September 23, 2017
Accepted: November 3, 2017
Published: November 3, 2017

DOI: 10.1021/acs.jpclett.7b02513
J. Phys. Chem. Lett. 2017, 8, 5695−5699

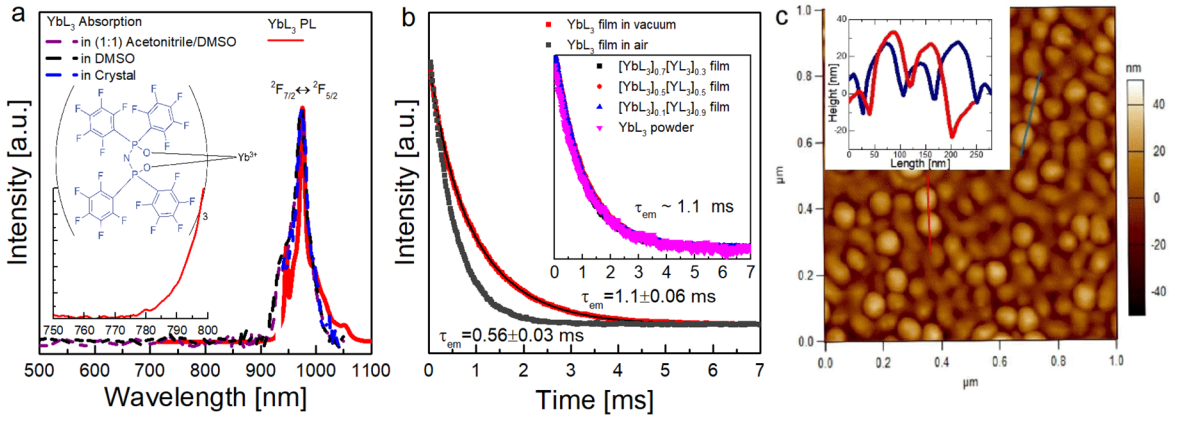

Figure 1. (a) Absorption in solution and solid and PL spectrum for YbL_3 powder, where L is F-TPIP$^-$. The wavelength region from 940 to 1050 nm was recorded at 910 nm excitation. The wavelength region from 700 to 900 nm shows the onset of Yb anti-Stokes emission at 975 nm excitation. (b) Time dependence of Yb PL using a 5 ns pulse at 975 nm excitation. The red dots for YbL_3 film emission in vacuum and the black solid is the fitting curve with a single-exponential function (details in the Supporting Information). The gray dots represent the spectrum data for the film emission exposed in air. The inset displays the corresponding Yb emission decays for $[YbL_3]_x[YL_3]_{1-x}$ (x = 0.1, 0.5, 0.7) films and YbL_3 powder. (c) AFM topography of a 200 nm thick $[YbL_3]_x[YL_3]_{1-x}$ film surface on a sapphire substrate in a 1 × 1 μm^2 area.

Organic materials usually have lower thermal conductivity [<1 W/(m-K)] than many oxides.[15] The interplay among them makes it interesting to consider organic lanthanide materials as a possibility in obtaining high-energy photons through thermal UC. However, difficulties will arise in the control of nonradiative channels, material stability, wavelength control, etc.

Herein, we first realize bright photon UC on organic lanthanide molecules through thermal and photoluminescence (PL) emission processes. We demonstrate that near-infrared (NIR)-emitting ytterbium (Yb) sensitizers that are chelated with perfluorinated organic ligands and the internal quantum yield (IQY) of Yb PL approaching unity cause terbium (Tb)-based molecule activators to incandesce brightly in the visible without significant losses. Moreover, the existence of a superimposed Tb UC permits a channel to further control the emission wavelength.

We have chosen tetrakis(pentafluorophenyl)imidodiphosphinimidic (F-TPIP$^-$) ligand (L$^-$) to obtain Yb, Tb, and Y complexes that are vacuum compatible to make integrated optic devices and can be incorporated in composite systems. The detailed material-related information can be found in the Supporting Information. In Figure 1a, the pristine YbL_3 absorption merely gives the peak at 975 nm wavelength, corresponding to the Yb $^2F_{7/2} \rightarrow 2F_{5/2}$ transition with no organic ligand absorption observed in the region. PL consists of an emission band from 780 to 1150 nm wavelengths, where the 780−830 nm wavelength region shows the tail of the anti-Stokes emission of $^2F_{5/2} \rightarrow {}^2F_{7/2}$ transition. Ligand shielding of Yb ions barely differs the complex absorption in solution and solid. Thus, we take the absorption spectrum in DMSO to calculate the radiative lifetime (τ_{rad}) of the Yb emission, which gives the τ_{rad}(solid) = 1.0 ± 0.2 ms taking into account the difference of refractive index[16] and the uncertainty of estimating the refractive index in the solid (section 4 of the Supporting Information).

The PL decay trace for the thin film placed in air, shown in Figure 1b, gives a Yb emission lifetime $\tau_{Yb(air)}$ = 0.56 ± 0.03 ms. However, the film placed in vacuum (<10^{-2} mbar) exhibits a long PL lifetime of 1.10 ± 0.06 ms (Figure S6). We ascribe the difference to the trapped trace H_2O molecules in air, which can permeate the space between the molecules (Figure 1c) through the small depth (20 nm) of the molecular grains observed in the morphological arrangement of the film. The result implies that the trace H_2O molecules of being not coordinated with the central ions are significant quenching centers for Yb emission. However, we find they desorb in vacuum, which facilely prevents this quenching. Moreover, this ∼1.1 ms lifetime is found to be sustainable with the Yb concentration diluted by optically inactive yttrium (Y) units in the series of $[YbL_3]_x[YL_3]_{1-x}$ (x = 0.7, 0.5, 0.1) (inset to Figure 1b). The unchanged lifetimes indicate that the Yb concentration quenching is very much reduced in the concentrated compound. We believe the reason is that the ligand shell isolates Yb ions from the quenching trap because of Yb ion concentration.[17,18]

The acquisition of the radiative lifetime and the PL lifetime gives a direct measurement of the internal quantum yield (IQY) of Yb emission. Given this, we estimate IQY = τ_{Yb}/τ_{rad} within the experimental error with a value approaching unity (>50% in air, > 86% in vacuum). The high IQY implies that direct vibrational quenching by the organic ligands is reduced. This elimination can be rationalized regarding the low phonon energies in the perfluorinated complex, and no evident vibration frequencies or overtones are detected >1650 cm^{-1} in the Fourier transform infrared spectrum of the complex (Figure S3).

To harvest Yb IR excitations, we chose the Tb ion as the activator. This choice is critical to realize bright UC because the Tb ion has no intermediate energy levels from the $^7F_{0-7}$ levels (<5000 cm^{-1}) to the $^5D_4$ level (∼20 000 cm^{-1}), and their energy gap ($\Delta E \geq$ 15 000 cm^{-1}) widely exceeds the F-TPIP$^-$ vibrational energies (>1650 cm^{-1}), while the intermediate ΔE among $^7F_{0-7}$ levels are well resonant with the organic vibrational energies. We employ $[YbL_3]_{0.7}[TbL_3]_{0.3}$, with the mixture ratio giving a Yb/Tb ratio of 2, which was reported to provide the most efficient CET UC in a Yb−Tb mixed system.[6,7] CET-induced Tb-based UC takes place with continuous-wave (CW) 975 nm excitation when the complex powder in vacuum (Figure S7), as allowed by the long Yb excited-state lifetime.

DOI: 10.1021/acs.jpclett.7b02513
J. Phys. Chem. Lett. 2017, 8, 5695−5699

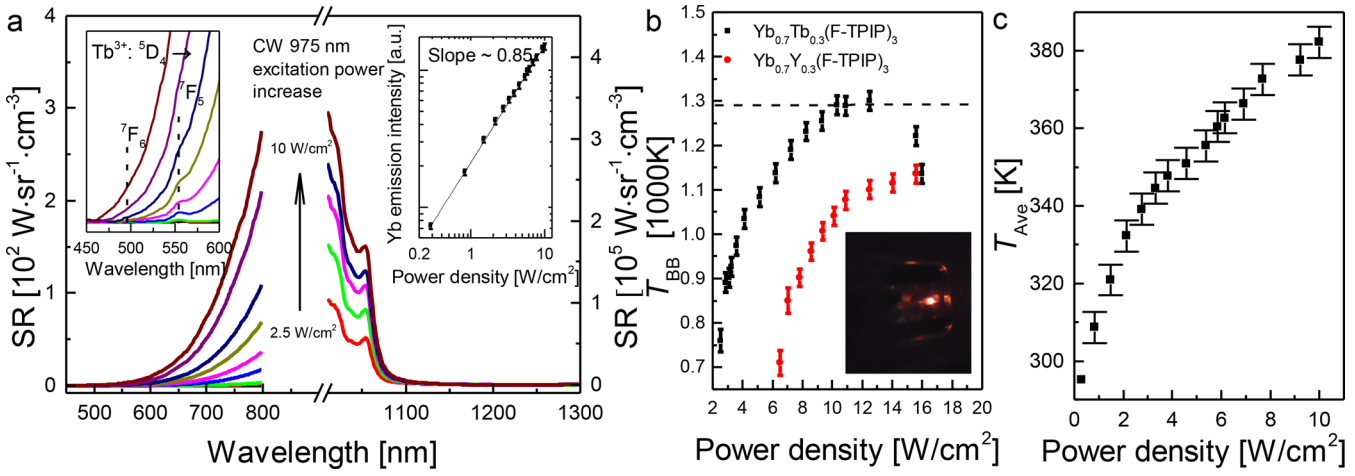

Figure 2. (a) Emission of $[YbL_3]_{0.7}[TbL_3]_{0.3}$ powder at 10^{-5} mbar vacuum taken at CW 975 nm excitation, where L is F-TPIP. The visible region (450−800 nm) primarily exhibits the visible fraction of the thermal radiation with the Tb emission peaks ($Tb^{3+5}D_4 \rightarrow {}^7F_{6,5}$) (zoom in, left inset). The NIR region (1010−1300 nm) primarily exhibits the conventional ytterbium emission. The power dependence of the integrated ytterbium emission intensities is plotted with logarithmic scale shown in the right inset. (b) Power dependence of the fitted T_{BB} for the thermal radiation after 975 nm excitation for $[YbL_3]_{0.7}[TbL_3]_{0.3}$ powder (black dots) and $[YbL_3]_{0.7}[YL_3]_{0.3}$ powder (red dots). The error bar is of ±20 K. The inset shows a picture of the visible fraction of the thermal radiation with 10 W/cm^2. The powder was mounted into a glass tube in a vacuum chamber. A 950 nm short-pass filter was employed to filter off laser scattering. (c) Estimated T_{Ave} of YbL_3 molecules in $[YbL_3]_{0.7}[TbL_3]_{0.3}$ composite system, derived from differential luminescence thermometry with an error bar of ±5K.

We then use high vacuum (~10^{-5} mbar) to further eliminate the permeated gas molecules, particularly trace H_2O and N_2, to reduce the thermal loss in the materials. This method is shown to be effective because Figure 2a shows a bright thermal UC for the sample in high vacuum, while the brightness decreases with the vacuum decreased. In high vacuum, the visible fraction rises when CW 975 nm excitation power increases from 2.5 to 10.0 W/cm^2 and gradually overwhelms the Tb UC (left inset to Figure 2a). Corresponding blackbody temperature (T_{BB}) can be obtained using the emission region (450−800 nm) by Planck's law fit, and the power dependence of the laser-induced T_{BB} is shown in Figure 2b. We found T_{BB} increases up to ~1300 K at 10 W/cm^2, while the T_{BB} and the spectral radiance (SR) intensity starts to drop after ~12.0 W/cm^2 due to the rapid material decomposition or evaporation.

Interestingly, the spectrum in the IR region from 1010 to 1300 nm wavelengths primarily exhibits the Yb emission of being much more intense than the IR fraction of the thermal radiation. Integrating Yb emission from 1010 to 1200 nm with the thermal radiation background subtracted remains roughly linear with power during the heating (right inset to Figure 2a) on a log scale power dependence plot. This linearity allows using differential luminescence thermometry (DLT)[19] (Figure S8) to estimate that the average temperature (T_{Ave}) of YbL_3 molecules, shown in Figure 2c, is increased only to a lower temperature of ~382 K within 0.3−10 W/cm^2. Replacing Tb with Y shows negligible thermal radiation in $[YbL_3]_{0.7}[YL_3]_{0.3}$ within higher excitation power (>7.8 W/cm^2) in Figure 2b, and the SR is at least 2 orders of the magnitude weaker than one for the $[YbL_3]_{0.7}[TbL_3]_{0.3}$ thermal UC at the same laser excitation level (Figure S9). Suppressed laser-induced heating on YbL_3 units and lower T_{Ave} can be expected because of the evidence of the eliminated nonradiative de-excitation directly from the Yb to organics. These data also make us believe that the thermal UC being localized on TbL_3 molecules is the key to reducing the excitation power of <10 W/cm^2, 1 order of magnitude lower than the reported excitation power for the thermal UC in inorganic oxides and comparable to that of the conventional lanthanide-based UC.[8,20,21] Low excitation power implies less solar concentration technology is required.

Figure 3 shows the time evolution of the dynamics and the energy migration routes. Yb PL decay trace in $[YbL_3]_{0.7}[TbL_3]_{0.3}$ with 0.79 ± 0.06 ms lifetime (5 ns pulse excitation) in vacuum becomes shorter than the pristine lifetime $\tau_{YbY(IR)}$ of ~1.1 ms, giving a CET rate estimate of $\tau_{Yb\rightarrow Tb(UC)}^{-1} = \tau_{YbTb(IR)}^{-1} - \tau_{YbY(IR)}^{-1} \approx 356\ s^{-1}$. Tb 550 nm emission peak shows a lifetime of 1.32 ± 0.07 ms (Figure 3) with the direct excitation (5 ns pulse excitation) into the Tb $^5D_4$ level, while Tb 550 nm UC (inset to Figure 3) shows a slightly shorter lifetime of 1.22 ± 0.07 ms with quasi-CW (38 ms square pulse) 975 nm excitation in vacuum. This might be due to the phonon-assisted energy migration between Tb ions enhanced by the laser-induced heating. Particularly, the interion interaction for the Tb ions could be dominant because the Tb emission lifetime is shorter than the reported one for TbL_3 dissolved in deuterated solvents.[22] The thermal UC has a rise time (20~45 ms) (Figure S10) longer than the one for Tb UC, which implies a thermal dissipation from beforehand-excited Tb units to Yb units to heat the materials to T_{Ave}. Nevertheless, it is likely that the thermal dissipation among molecular clusters is disrupted because of the ~20 nm vacuum space between grains, which could reduce the thermal loss from the high-temperature centers to the neighboring ones. This might explain the rise time being much shorter than those (from seconds to minutes) in crystalline or nanocrystalline oxides, which have higher thermal conductivity benefiting thermal dissipation over bulky hosts.[9,12] Our discovered phenomena thus are distinct from the thermal UC in lanthanide-doped inorganics, where the sensitizers and host have no temperature difference.

According to themethod reported in literature,[8] we can estimate the emission quantum efficiency (QE) for the process: QE = 0.13% at 975 nm excitation with 10 W/cm^2 from the ratio of the integrated band radiance to the integrated spectral radiance. Our thermal UC QE is limited by the maximum reachable blackbody temperature that is lower than ~2100 K reached in inorganics.[8,9] However, the low excitation power can

DOI: 10.1021/acs.jpclett.7b02513
J. Phys. Chem. Lett. 2017, 8, 5695−5699

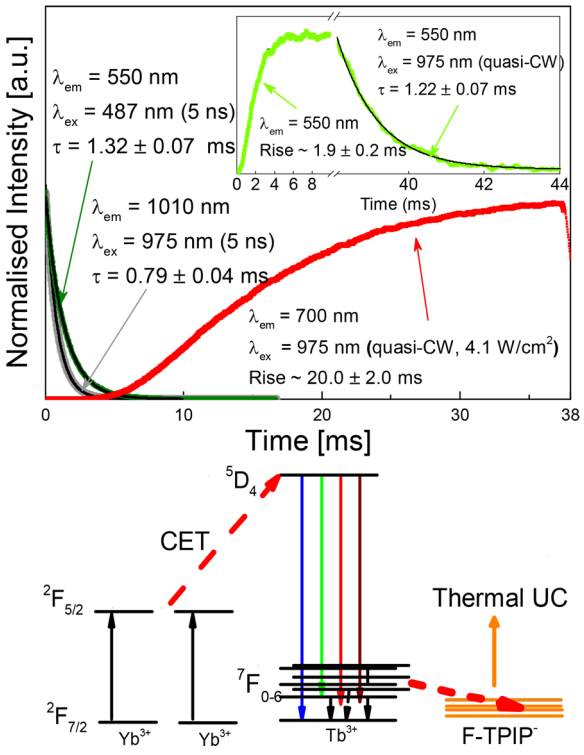

Figure 3. Time evolution of photon emission in $[YbL_3]_{0.7}[TbL_3]_{0.3}$ powder: Yb PL (gray dots) for 975 nm excitation using a 5.0 ns pulse. Tb^{3+}:$^5D_4 \rightarrow {}^7F_5$ emission (dark green dots) when directly excited to $^5D_4$ level using a 5 ns pulse at 487 nm excitation. Tb^{3+}:$^5D_4 \rightarrow {}^7F_5$ emission (green dots, the inset) when excited using a square 38.0 ms pulse at 975 nm excitation. Fitting curves (black lines) are using single-exponential functions (details in the Supporting Information). The thermal UC recorded at 700 nm wavelength (red curve) when excited using a square 38.0 ms pulse at 975 nm excitation. The time values resulted from the fit of the exponential functions. Jablonski diagram (below) detailing the energy-transfer processes among Yb, Tb, and organic vibrations. Dashed arrows represent nonradiative processes, and colored solid arrows represent the absorption and emission of photon. The red dashed arrows represent the CET from Yb^{3+}:$^2F_{5/2}$ to Tb^{3+}:$^5D_4$ and multiphonon-relaxation from Tb to organic vibrations. The black dashed arrows represent nonradiative deactivations in Tb^{3+} transitions.

give a normalized QE of 1.33×10^{-4} cm^2/W at 1300 K, which is comparable to those achieved in the UC of inorganics.[8] The stability of the organic materials containing aromatic rings up to the ~1200 K has been reported even in a hydrogenated organic metallic complex such as copper phthalocyanine in vacuum.[23,24] Also, perfluorinated materials are known to have much higher thermal stability in general.[25,26] In our studied complexes, the overall effect of the coordinated perfluorinated aromatic rings of $-(C_6F_5)$, the ring configuration of $-(O-P-N-P-O)-$, and the high geometric symmetry of the complex molecule[27] could further enhance the thermal stability. In fact, investigating the time-stability of the thermal radiation in $[YbL_3]_{0.7}[TbL_3]_{0.3}$ indicates the unchanged chemical composition of the material at the available level of detection (details in section 8 of the Supporting Information).

We have unprecedentedly realized the bright photon UC on organic lanthanide molecules in the solid state by engineering the dynamic pathways among the Yb sensitizers, Tb activators, and organic ligands. The temperature difference between the sensitizers and activators in the composite is first demonstrated, owing to the ultrahigh IQY of Yb emission in the pristine Yb perfluorinated complex. The results imply a novel enery material system allowing for improved convenience and compatibility for integrating a photon UC layer onto thermal PV devices.

EXPERIMENTAL METHODS

Details of experimental methods in material synthesis, optical characterization, and data analysis are available in the Supporting Information. In summary, tetrakis(pentafluorophenyl)imidodiphosphinate acid (>98% Changzhou Garde Pharmtech Co. Ltd., China) and the lanthanide chlorides (>99.99% Sigma-Aldrich) are commercially purchased. Materials are purified using vacuum train purification prior to the use for experiments. Film samples are fabricated using a high-vacuum deposition system. $B(\lambda, T_{BB}) = \left(\frac{2h^2}{\lambda^5}\right)(e^{hc/\lambda k_B T} - 1)$ according to Planck's law was used to fit thermal radiation spectra to yield T_{BB} with $R^2 > 0.99$. Exponential functions were used for lifetime fitting. A homemade vacuum chamber was used to place the materials in vacuum.

ASSOCIATED CONTENT

Supporting Information

The Supporting Information is available free of charge on the ACS Publications website at DOI: 10.1021/acs.jpclett.7b02513.

Method to obtain luminescence spectra, thin-film preparation, detailed materials characterization, IQYs calculation methods, data analysis for time-resolved measurements, additional spectral data for UC and thermal radiation, and thermal stability studies (PDF)

AUTHOR INFORMATION

Corresponding Author

*E-mail: qihua@ntu.edu.sg.

ORCID

Huanqing Ye: 0000-0002-7737-2676
Ignacio Hernández: 0000-0001-7104-8907
Qihua Xiong: 0000-0002-2555-4363

Notes

The authors declare no competing financial interest.

ACKNOWLEDGMENTS

Q.X. acknowledges the support from the Singapore National Research Foundation through Investigatorship award (NRF-NRFI2015-03), and the Singapore Ministry of Education via an AcRF Tier 2 grant (MOE2013-T2-1-049) and a Tier 1 grants (2015-T1-001-175 and RG113/16). I.H. acknowledges EU FP7 (MC-CIG Grant 303535) and Spanish MINECO (Grant MAT2016-80438-P).

REFERENCES

(1) Wang, H.; Batentschuk, M.; Osvet, A.; Pinna, L.; Brabec, C. J. Rare-Earth Ion Doped Up-Conversion Materials for Photovoltaic Applications. *Adv. Mater.* **2011**, *23*, 2675−2680.

(2) Yu, M.; Qu, Y.; Pan, K.; Wang, G.; Li, Y. Enhanced Photoelectric Conversion Efficiency of Dye-Sensitized Solar Cells by the Synergetic Effect of $NaYF_4$:Er^{3+}/Yb^{3+} and G-C_3N_4. *Sci. China Mater.* **2017**, *60*, 228−238.

(3) Haase, M.; Schäfer, H. Upconverting Nanoparticles. *Angew. Chem., Int. Ed.* **2011**, *50*, 5808−5829.

DOI: 10.1021/acs.jpclett.7b02513
J. Phys. Chem. Lett. 2017, 8, 5695−5699

(4) Gargas, D. J.; Chan, E. M.; Ostrowski, A. D.; Aloni, S.; Altoe, M. V. P.; Barnard, E. S.; Sanii, B.; Urban, J. J.; Milliron, D. J.; Cohen, B. E.; et al. Engineering Bright Sub-10-Nm Upconverting Nanocrystals for Single-Molecule Imaging. *Nat. Nanotechnol.* **2014**, *9*, 300−305.
(5) Salley, G. M.; Valiente, R.; Güdel, H. U. Cooperative Yb^{3+}− Tb^{3+} Dimer Excitations and Upconversion in $Cs_3Tb_2Br_9$: Yb^{3+}. *Phys. Rev. B: Condens. Matter Mater. Phys.* **2003**, *67*, 134111.
(6) Hernández, I.; Pathumakanthar, N.; Wyatt, P. B.; Gillin, W. P. Cooperative Infrared to Visible Up Conversion in Tb^{3+}, Eu^{3+}, and Yb^{3+} Containing Polymers. *Adv. Mater.* **2010**, *22*, 5356−5360.
(7) Souri, N.; Tian, P.; Platas-Iglesias, C.; Wong, K.-L.; Nonat, A.; Charbonnière, L. J. Upconverted Photosensitization of Tb Visible Emission by NIR Yb Excitation in Discrete Supramolecular Heteropolynuclear Complexes. *J. Am. Chem. Soc.* **2017**, *139*, 1456−1459.
(8) Wang, J.; Ming, T.; Jin, Z.; Wang, J.; Sun, L.-D.; Yan, C.-H. Photon Energy Upconversion through Thermal Radiation with the Power Efficiency Reaching 16%. *Nat. Commun.* **2014**, *5*, 5669.
(9) Soares, M. R. N.; Ferro, M.; Costa, F. M.; Monteiro, T. Upconversion Luminescence and Blackbody Radiation in Tetragonal YSZ Co-Doped with Tm^{3+} and Yb^{3+}. *Nanoscale* **2015**, *7*, 19958−19969.
(10) Bierman, D. M.; Lenert, A.; Chan, W. R.; Bhatia, B.; Celanović, I.; Soljačić, M.; Wang, E. N. Enhanced Photovoltaic Energy Conversion Using Thermally Based Spectral Shaping. *Nat. Energy* **2016**, *1*, 16068.
(11) Boriskina, S. V.; Chen, G. Exceeding the Solar Cell Shockley−Queisser Limit via Thermal up-Conversion of Low-Energy Photons. *Opt. Commun.* **2014**, *314*, 71−78.
(12) Chen, Z.; Jia, H.; Sharafudeen, K.; Dai, W.; Liu, Y.; Dong, G.; Qiu, J. Up-Conversion Luminescence from Single Vanadate through Blackbody Radiation Harvesting Broadband near-Infrared Photons for Photovoltaic Cells. *J. Alloys Compd.* **2016**, *663*, 204−210.
(13) Bünzli, J.-C. G. On the Design of Highly Luminescent Lanthanide Complexes. *Coord. Chem. Rev.* **2015**, *293−294*, 19−47.
(14) Tan, R. H. C.; Motevalli, M.; Abrahams, I.; Wyatt, P. B.; Gillin, W. P. Quenching of IR Luminescence of Erbium, Neodymium, and Ytterbium β-Diketonate Complexes by Ligand CH and CD Bonds. *J. Phys. Chem. B* **2006**, *110*, 24476−24479.
(15) Kim, N.; Domercq, B.; Yoo, S.; Christensen, A.; Kippelen, B.; Graham, S. Thermal Transport Properties of Thin Films of Small Molecule Organic Semiconductors. *Appl. Phys. Lett.* **2005**, *87*, 241908.
(16) Shavaleev, N. M.; Scopelliti, R.; Gumy, F.; Bünzli, J.-C. G. Surprisingly Bright Near-Infrared Luminescence and Short Radiative Lifetimes of Ytterbium in Hetero-Binuclear Yb− Na Chelates. *Inorg. Chem.* **2009**, *48*, 7937−7946.
(17) Johnson, N. J. J.; He, S.; Diao, S.; Chan, E. M.; Dai, H.; Almutairi, A. Direct Evidence for Coupled Surface and Concentration Quenching Dynamics in Lanthanide-Doped Nanocrystals. *J. Am. Chem. Soc.* **2017**, *139*, 3275−3282.
(18) Hernández, I.; Zheng, Y.-X.; Motevalli, M.; Tan, R. H. C.; Gillin, W. P.; Wyatt, P. B. Efficient Sensitized Emission in Yb (III) Pentachlorotropolonate Complexes. *Chem. Commun.* **2013**, *49*, 1933−1935.
(19) Seletskiy, D. V.; Melgaard, S. D.; Bigotta, S.; Di Lieto, A.; Tonelli, M.; Sheik-Bahae, M. Laser Cooling of Solids to Cryogenic Temperatures. *Nat. Photonics* **2010**, *4*, 161−164.
(20) Hyppänen, I.; Lahtinen, S.; Ääritalo, T.; Mäkelä, J.; Kankare, J.; Soukka, T. Photon Upconversion in a Molecular Lanthanide Complex in Anhydrous Solution at Room Temperature. *ACS Photonics* **2014**, *1*, 394−397.
(21) Suffren, Y.; Golesorkhi, B.; Zare, D.; Guénée, L.; Nozary, H.; Eliseeva, S. V.; Petoud, S.; Hauser, A.; Piguet, C. Taming Lanthanide-Centered Upconversion at the Molecular Level. *Inorg. Chem.* **2016**, *55*, 9964−9972.
(22) Glover, P. B.; Bassett, A. P.; Nockemann, P.; Kariuki, B. M.; Van Deun, R.; Pikramenou, Z. Fully Fluorinated Imidodiphosphinate Shells for Visible-and NIR-Emitting Lanthanides: Hitherto Unexpected Effects of Sensitizer Fluorination on Lanthanide Emission Properties. *Chem. - Eur. J.* **2007**, *13*, 6308−6320.
(23) Erk, P.; Hengelsberg, H. 119 - Phthalocyanine Dyes and Pigments. In *The Porphyrin Handbook*; Kadish, K. M., Smith, K. M., Guilard, R., Eds.; Academic Press: Amsterdam, 2003; pp 105−149.
(24) Lawton, E. A. The Thermal Stability of Copper Phthalocyanine. *J. Phys. Chem.* **1958**, *62*, 384.
(25) Johns, I. B.; McElhill, E. A.; Smith, J. O. Thermal Stability of Organic Compounds. *Ind. Eng. Chem. Prod. Res. Dev.* **1962**, *1*, 2−6.
(26) Johns, I. B.; McElhill, E. A.; Smith, J. O. Thermal Stability of Some Organic Compounds. *J. Chem. Eng. Data* **1962**, *7*, 277−281.
(27) Ye, H.-Q.; Peng, Y.; Li, Z.; Wang, C.-C.; Zheng, Y.-X.; Motevalli, M.; Wyatt, P. B.; Gillin, W. P.; Hernández, I. Effect of Fluorination on the Radiative Properties of Er^{3+} Organic Complexes: An Opto-Structural Correlation Study. *J. Phys. Chem. C* **2013**, *117*, 23970−23975.

DOI: 10.1021/acs.jpclett.7b02513
J. Phys. Chem. Lett. 2017, 8, 5695−5699